The time course of ongoing activity during neuritis and following axonal transport disruption

Article (Accepted Version)

TITLE

The time course of ongoing activity during neuritis and following axonal transport disruption

AUTHORS

Ieva Satkeviciute[A], George Goodwin[A], Geoffrey M Bove[B], Andrew Dilley[A]

AFFILIATIONS

[A] Brighton and Sussex Medical School, University of Sussex, Brighton BN1 9PS, UK

[B] University of New England, Biddeford, Maine, USA

RUNNING HEAD

Axonal transport disruption-induced ectopic activity

CORRESPONDING AUTHOR:

Dr Andrew Dilley PhD

Department of Neuroscience,

Brighton and Sussex Medical School,

Medical Research Building,

University of Sussex,

Falmer,

Brighton BN1 9PS,

United Kingdom

Tel: +44 (0) 1273 877094

Fax: +44 (0) 1273 877884

Email: a.dilley@bsms.ac.uk

ABSTRACT

Local nerve inflammation (neuritis) leads to ongoing activity and axonal mechanical sensitivity (AMS) along intact nociceptor axons, and disrupts axonal transport. This phenomenon forms the most feasible cause of radiating pain, such as sciatica. We have previously shown that axonal transport disruption without inflammation or degeneration also leads to AMS, but does not cause ongoing activity at the time point when AMS occurs, despite causing cutaneous hypersensitivity. However, there have been no systematic studies of ongoing activity during neuritis or non-inflammatory axonal transport disruption. In this study, we present the time course of ongoing activity from primary sensory neurons following neuritis and vinblastine-induced axonal transport disruption. Whereas 24% of C/slow Aδ-fiber neurons had ongoing activity during neuritis, few (<10%) A- and C-fiber neurons showed ongoing activity 1-15 days following vinblastine treatment. In contrast, AMS increased transiently at the vinblastine treatment site, peaking on day 4-5 (28% of C/slow Aδ-fiber neurons) and resolved by day 15. Conduction velocities were slowed in all groups. In summary, the disruption of axonal transport without inflammation does not lead to ongoing activity in sensory neurons, including nociceptors, but does cause a rapid and transient development of AMS. Since it is proposed that AMS underlies mechanically-induced radiating pain, and a transient disruption of axonal transport (as previously reported) leads to transient AMS, it follows that processes that disrupt axonal transport, such as neuritis, must persist to maintain AMS and the associated symptoms.

NEW AND NOTEWORTHY

Many patients with radiating pain lack signs of nerve injury on clinical examination, but may have neuritis, which disrupts axonal transport. We have shown that axonal transport disruption does not induce ongoing activity in primary sensory neurons but does cause transient axonal mechanical sensitivity. The present data complete a profile of key axonal sensitivities following axonal transport disruption. Collectively, this profile supports that an active peripheral process is necessary for maintained axonal sensitivities.

KEYWORDS

Axonal transport disruption, vinblastine, ongoing activity, axonal mechanical sensitivity, neuropathic pain

INTRODUCTION

Conditions that cause radiating pain remain prevalent. Examples of such conditions include non-specific arm or back pain, sciatica, fibromyalgia, whiplash associated disorder, diabetes, complex regional pain syndrome, and endometriosis (Dilley and Greening 2012; Dyck et al. 2000; Janig and Baron 2003; Loeser 1985; Waddell 1987; Woertgen et al. 1998; Zager et al. 1998). Many of these patients lack signs of a nerve injury on clinical examination. Instead, these patients may have inflamed nerves (i.e. neuritis) that are otherwise intact and are considered normal using typical clinical tests. Magnetic resonance imaging studies in some of these patients have identified increases in T2-weighted signal intensity along nerve trunks that are consistent with neuritis (Dilley et al. 2011; Greening et al. 2018).

A rat model of neuritis has given much of our understanding about the mechanisms that underlie pain in these patients. In this model, animals develop transient behavioral sensory hypersensitivities to tactile and thermal stimuli in the absence of axonal degeneration (Bove et al. 2003; Chacur et al. 2001; Eliav et al. 1999; Pulman et al. 2013). At some time points following neuritis induction, the axons of intact nociceptors fire spontaneously, respond to direct mechanical stimulation at the site of inflammation (Bove et al. 2003; Dilley et al. 2005; Richards and Dilley 2015), and become sensitive to noxious inflammatory chemicals (Govea et al. 2017). Such ectopic activity and sensitivity constitute the most feasible source of afferent nociceptor activity contributing to spontaneous pain and mechanically-evoked radiating pain that are reported in patients in the absence of nerve injury (Dilley and Greening 2012). This activity may also contribute to the afferent barrage that is reputed to drive central mechanisms that cause cutaneous hypersensitivities (Campbell and Meyer 2006; Gracely et al. 1992; Woolf 2011; Xie et al. 2005).

We have shown that neuritis disrupts fast axonal transport along intact sensory axons, and that such disruption leads to axonal sensitivities (Dilley and Bove 2008a; Dilley et al. 2013). We have

hypothesized that the mechanisms underlying these sensitivities involve the accumulation and insertion of ion channels at the site of disruption. The effects of axonal transport disruption along intact axons can be examined by applying low doses of the vinca alkaloid, vinblastine, to the rat sciatic nerve (Dilley and Bove 2008a; Fitzgerald et al. 1984). At low doses, perineural vinblastine disrupts microtubule polymerization without causing axonal degeneration or inflammation (Dilley and Bove 2008a; Fitzgerald et al. 1984; Kashiba et al. 1992; Katoh et al. 1992; Zhuo et al. 1995), which allows axonal transport disruption to be examined in the absence of these potentially confounding factors. Using this model, we have shown that localized vinblastine treatment causes the development of a transient tactile-evoked cutaneous hypersensitivity (Dilley et al. 2013). At approximately the peak of this pain behavior (day 4-5), intact C-fiber neurons develop axonal mechanical sensitivity (AMS) at the treatment site (Dilley and Bove 2008a; Dilley et al. 2013). In a previous study, ongoing activity from A- or C- fiber axons was not increased at this time point, which contrasts from neuritis and nerve injury models where it is a major feature (Boucher et al. 2000; Bove and Dilley 2010; Kajander et al. 1992; Tal and Eliav 1996).

Both neuritis and vinblastine-induced axonal transport disruption are short-lived phenomena (Bove et al. 2009; Dilley et al. 2013), but patient symptoms are often chronic. This inconsistency has led to the suggestion that patients may have a persistent peripheral stimulus. To determine whether such altered nociceptor activities require an active stimulus, we have performed a detailed assessment of the time course of ongoing activity in these models. We also present the temporal profile of vinblastine-induced AMS, to compare with the ongoing activity. Together, the data from the present and past experiments complete the profile of ectopic activity and sensitivity, which informs peripheral mechanisms of radiating pain.

METHODS

Animals and surgery

Experiments were carried out in strict accordance with the UK Animals (Scientific Procedures) Act (1986) and Home Office guidelines. Formal approval was also obtained from the University of Sussex Animal Welfare Ethical Review Board. Adult male Sprague Dawley rats (n = 62; 250-500 g; Charles River Laboratories, Kent, UK) were used in this study. Rats were given ad libitum access to food and water. Animals were monitored daily.

Vinblastine was applied to the sciatic nerve of adult rats (n = 32) as previously described (Dilley and Bove 2008a). Under general anesthesia (1.75% isoflurane in oxygen), the left sciatic nerve was exposed by blunt dissection. An 8 mm length was cleared from its connective tissue, which allowed a short length of sterile parafilm (6 x 20 mm; Sigma Aldrich, Dorset, UK) to be positioned under the nerve to prevent leakage of vinblastine onto the surrounding tissue. The sciatic nerve was loosely wrapped with a strip of sterile Gelfoam (5 x 5 x 10 mm; Spongostan^{TM}; Ferrosan, Denmark) saturated in 0.1 mM vinblastine (Sigma Aldrich, Dorset, UK; diluted 0.9% w/v saline). Both the Gelfoam and parafilm were removed after 15 min. The nerve was thoroughly rinsed with sterile saline and the muscle and skin were closed using 4/0 monofilament sutures (Vicryl; Ethicon, West London, United Kingdom). The saline group (n = 9) underwent identical surgery, but instead the Gelfoam was saturated with 0.9% w/v saline alone.

Neuritis was induced as previously described (n = 13) (Dilley and Bove 2008b). The left sciatic nerve was exposed by blunt dissection and an 8 mm length was cleared from the surrounding connective tissue. A sterile strip of Gelfoam (5 x 5 x 10 mm) saturated in 50% complete Freund's adjuvant (diluted in sterile 0.9% w/v saline) was loosely wrapped around the nerve. The muscle and skin were closed using 4/0 monofilament sutures.

Electrophysiology

Single-unit extracellular electrophysiological recordings were made from A- and C-fiber axons in the L5 dorsal root as previously described (Bove et al. 2003). The L5 dorsal root innervates much of the plantar surface of the foot that was examined during behavioral testing. Experiments were carried out at 2 hours to 15 days following vinblastine treatment (n = 32), neuritis (n = 13) and saline treatment (n = 9), and in untreated animals (n = 9). Briefly, animals were deeply anesthetized (1.5 g/kg 25% w/v urethane intraperitoneally) and the body temperature was maintained at 37°C using a rectal thermistor probe attached to a feedback controlled heat mat (Harvard Apparatus, Kent, UK). A mid-sagittal skin incision was made in the lumbar region of the back and a laminectomy was performed from the L2 to L5 vertebrae. The surrounding skin was sutured to a metal ring to form a pool. The dura mater was cut to expose the caudal end of the spinal cord and cauda equina, and the pool was filled with mineral oil warmed to 37°C. The temperature of the pool was monitored during each experiment and was topped up with warmed mineral oil when necessary. The ipsilateral L5 dorsal root was identified and cut just before it enters the spinal cord, and loosely placed onto a glass platform (9 mm x 5 mm). Individual fine filaments were teased from the cut end of the nerve with finely sharpened forceps and carefully positioned on a bipolar recording electrode. In the mid-thigh, the sciatic nerve was exposed and the surrounding skin flaps were stitched to a metal ring to form a second mineral oil pool. Ongoing activity and AMS were assessed in different animals because repeated mechanical stimulation of the sciatic nerve at the treatment site can lead to the development of ongoing activity (Dilley et al. 2005). Receptive fields were also not examined during experiments to assess levels of ongoing activity, since noxious mechanical stimulation that is necessary to activate the terminals of nociceptors can cause ongoing activity (Bove and Dilley 2010; Richards et al. 2011).

158 To measure C-fiber conduction velocities (<2 m/s), a bipolar stimulating electrode was positioned
159 under the L5 dorsal root, and activity evoked by electrical stimulation using a constant-voltage
160 isolated stimulator (square wave pulses; 0.5 ms duration, 30-50 V amplitude; Digitimer,
161 Hertfordshire, United Kingdom). We have previously confirmed that the majority of neurons in the
162 L5 dorsal root conduct through the sciatic nerve in the mid-thigh (i.e. through the treatment site)
163 (Dilley et al. 2013). To measure A-fiber conduction velocities (>2 m/s), bipolar stimulating electrodes
164 were positioned under the sciatic nerve immediately distal to the treatment site, and activity evoked
165 by electrical stimulation at this site (square wave pulses; 0.05 ms duration, 3-10 V amplitude). During
166 these stimuli, the limb was held in place by a noose around the foot. It should be noted that
167 muscular contractions of the foot during electrical stimulation at A-fiber strength were only small,
168 whereas stimulation at C-fiber strength would lead to substantial movement artifacts. The long
169 conduction distance (range: 61-88 mm) allowed identification of individual A-fiber neurons. For each
170 recording, the amplitude of the electrical stimulus was increased until the maximum number of
171 waveforms was evoked. Only neurons with easily identifiable waveforms were examined. The
172 number of waveforms on each filament ranged from 1 to 7. Action potentials were amplified (1-2 K),
173 band-pass filtered (10-5000 Hz) and monitored with an oscilloscope. Neuronal activity was digitized,
174 recorded and analyzed with Spike 2 software (Cambridge Electronic Designs, Cambridge, UK). At the
175 end of an experiment, the sciatic nerve and L5 dorsal root were removed and the conduction
176 distance was measured. Conduction velocities of each neuron were calculated from the conduction
177 latency and conduction distance.

178 In experiments to evaluate ongoing activity, identified neurons were recorded for 3 min. Neurons
179 that fired at least once per minute were considered to exhibit ongoing activity (Bove and Dilley
180 2010). Muscle spindles, identified by high frequency position- and movement-dependent repetitive
181 firing, were excluded from the data analysis. Neurons with ongoing activity were identified as either
182 A- or C-fiber neurons by spike shape. C-fiber neurons typically had a longer duration and were often
183 biphasic compared to A-fiber neurons, which were monophasic (Dilley et al. 2005).

In the experiments to evaluate AMS, A-fiber neurons were not examined, since AMS in the Aβ population is rarely observed following vinblastine treatment (unpublished observations) or in the neuritis model (Bove et al. 2003). In the thigh, the sciatic nerve was exposed and a plastic platform (9 mm × 5 mm), notched to accommodate the nerve, was placed under the nerve with the treatment site in its center. Receptive fields for isolated neurons were searched below the knee using mechanical stimuli. Most receptive fields were located by squeezing the periphery, using either fingers or forceps. The loose property of the skin was exploited to carefully discriminate cutaneous *versus* deep fields (Bove et al. 2003). Cutaneous neurons had receptive fields that remained associated with the skin, whereas deep neurons (i.e. neurons that innervate muscles, tendons and joints) had receptive fields that remained in the same underlying spot irrespective of the skin position. For example, if a neuron responded to pinching a fold of skin, and maintained similar responsiveness when this fold was displaced, it was concluded that its receptive field was cutaneous. In contrast, if the repeated application of the effective stimulus to same underlying point produced a similar neuronal response despite displacement of the overlying skin, it was concluded that the receptive field was deep (e.g. in muscle). After identification of a receptive field, the conduction velocity of the neuron was determined by electrically stimulating the dorsal root while mechanically stimulating the receptive field. If the neuron fired to mechanically-evoked stimulation of the receptive field immediately prior to the electrical stimulation of the nerve, the same neuron evoked by the electrical stimulus would be delayed or would not be initiated (i.e. the electrical stimulus occurred during the refractory period).

Mechanical stimulation of the nerve was manually applied using a silicone probe as previously described (Bove et al. 2003; Dilley and Bove 2008a; b). The tip of the probe was conical shaped and cut at the end to form a flat footprint approximately 5 x 3.5 mm. The mechanical stimulus was applied for 1-2 sec successively along the length of nerve that was located on the notched platform (i.e. the treatment site or equivalent length in untreated animals). The force applied with the probe was <20 cN (as measured on an electronic scale). Using the probe in this manner does not interrupt

the conduction of action potentials (i.e. cause damage to axons), confirmed by repeated activation of each neuron at its receptive field following axonal mechanical sensitivity testing. The conduction velocity of axons that were mechanically sensitive was determined by electrically stimulating the dorsal root while mechanically stimulating the treatment site as described above.

Data analysis

Data were tested for normality using Shapiro-Wilk tests. Comparisons between the proportions of neurons with ongoing activity or AMS were made using Fisher's exact tests. Conduction velocities of A- and C-fiber neurons and rates of ongoing activity from C-fiber neurons were compared between time points and to saline treatment using Kruskal-Wallis tests followed by Dunn's post hoc tests. Due to the small number of A-fiber neurons with ongoing activity, rates could not be statistically compared. Comparisons of conduction velocities between neurons with and without AMS were made using Mann-Whitney tests. Conduction velocities and rates of ongoing data are presented as median +/- interquartile range (IQR).

RESULTS

Conduction velocities

Conduction velocity data are summarized in Fig. 1. Recordings were made from a total of 2124 neurons in the L5 dorsal root following vinblastine, neuritis, and saline treatment, and in untreated animals. Histograms of the conduction velocities are shown in Fig. 1A and B. Based on the conduction velocities, neurons were characterized as either C/slow Aδ- (0.2-2.1 m/s; n = 1212) or Aα/β-fiber neurons (>10 m/s; n = 912) (Waddell et al. 1989).

In the untreated group, the median conduction velocity of the C/slow Aδ- fiber neurons was 0.58 m/s (IQR = 0.29; combined data from AMS and ongoing activity experiments). Following vinblastine treatment, neuritis and saline treatment, there was a significant slowing of conduction 3-4 hours postoperative compared to the untreated group ($p < 0.05$, Kruskal-Wallis test; $p < 0.001$, Dunn's post hoc tests). In the vinblastine treated group, conduction was also slowed at 4-5 and 12-15 days following surgery ($p < 0.05$, Dunn's post hoc tests). Following neuritis, conduction was slowed at all of the time points examined ($p < 0.01$, Dunn's post hoc tests). The maximum slowing was at 3-4 hours postoperative following vinblastine treatment (19.7% compared to untreated; median = 0.47 m/s (IQR = 0.16)) and neuritis (41.2% compared to untreated; median = 0.34 m/s (IQR = 0.22); Fig. 1C).

In the untreated group, the median conduction velocity of the Aα/β-fiber neurons was 33.01 m/s (IQR = 12.78). Following both vinblastine and saline treatment, the conduction velocities of the Aαβ-fiber neurons were comparable to the untreated group at the time points examined. Following neuritis, conduction velocities were significantly reduced at 3-4 hours and 1-2 days postoperative ($p < 0.05$, Kruskal-Wallis test; $p < 0.01$, Dunn's post hoc tests). The maximum reduction was at 3-4 hours following treatment (20.8% compared to untreated; median = 26.16 m/s (IQR = 8.81) Fig. 1D).

Ongoing activity

The proportion of C/slow Aδ-fiber neurons in each group with ongoing activity is summarized in Fig. 2A. Ongoing activity developed in 5.3% of C/slow Aδ-fiber neurons in the untreated group, with a median firing rate of 0.60 (IQR = 1.03) Hz. Following vinblastine treatment, the proportions of C/slow Aδ-fiber neurons with ongoing activity ranged from 6.0 to 10.8% at the time points examined, which were not significantly different from the untreated group ($p > 0.24$, comparing individual time points to untreated) or following saline treatment ($p > 0.12$ at 3-4 hours and 4-5 days postoperative, Fisher's exact tests). The median rate of ongoing activity in these neurons was < 0.35Hz, which was comparable between time points ($p = 0.21$, Kruskal-Wallis test; Table 1). In contrast to vinblastine treatment, there was a significant increase in ongoing activity from C/slow Aδ- fiber neurons following neuritis on day 4-5 postoperative, with 23.9% (21/88) of neurons firing spontaneously ($p<0.05$ Fisher's exact test, compared to untreated and saline-treated). The rates of ongoing activity following neuritis at 1-2 days postoperative were significantly increased compared to 3-4 hours and 12-15 days postoperative ($p < 0.05$, Kruskal-Wallis test; $p <0.05$, Dunn's post hoc tests). The firing patterns were all irregular (e.g. Fig. 2B).

The proportion of Aα/β-fiber neurons in each group with ongoing activity is summarized in Fig. 3A. Ongoing activity was present in only 1 Aα/β-fiber neuron (1.3%, 1/79 neurons) in the untreated group, which had an irregular slow (0.02 Hz) firing pattern (Fig. 4B). Following vinblastine treatment, ongoing activity was observed in 1.1 to 5.3% of Aα/β-fiber neurons at the time points examined, which was not significantly different from the untreated group ($p > 0.20$ comparing individual time points to untreated) or to saline treatment ($p > 0.68$ at 3-4 hours and 4-5 days postoperative, Fisher's exact tests). Following neuritis, ongoing activity was observed in 1.3 to 6.5% of Aα/β-fiber neurons, which was also not significantly different from the untreated group ($p > 0.14$ comparing individual time points to untreated) or to saline treatment ($p > 0.44$ at 3-4 hours and 4-5 days

postoperative, Fisher's exact tests). Median rates of ongoing activity in all Aα/β-fiber neurons were low (median rate < 0.24 Hz; Table 1). Firing patterns were all irregular (e.g. Fig. 3B).

Axonal mechanical sensitivity

The proportion of C/slow Aδ-fiber neurons in each group with deep and cutaneous receptive fields that developed AMS is summarized in Fig. 4. All of the neurons had receptive fields below the knee. The receptive fields of each of these neurons had a high mechanical threshold, responding to firm squeezing of the receptive field. Axonal mechanical sensitivity testing was repeatable and activation of the receptive field before and following testing confirmed that the axons remained intact. The majority of AMS 'hotspots' were either immediately proximal to, or at, the treatment site. No AMS 'hotspots' were found distally. AMS did not develop in the untreated (0/28 neurons) or saline-treated groups (0/23 neurons). Following vinblastine treatment, AMS was detected only in neurons with deep receptive fields (i.e. in muscles or joints), that is, none of the neurons with cutaneous receptive fields exhibited AMS. Axonal mechanical sensitivity developed rapidly, with 15.8% (6/38) of all C-fiber neurons responding to direct mechanical stimulation at the treatment site on day 1-2 postoperative ($p<0.05$ compared to untreated (0/28), Fisher's exact test). The proportion of neurons with AMS reached a maximum on day 4-5, with 27.6% (8/29) of all neurons responding to mechanical stimulation ($p<0.01$ and $p<0.05$ compared to untreated and saline-treated on day 4-5 postoperative (0/23) respectively, Fisher's exact test). On day 8-9, 8.3% (2/24) of all neurons developed AMS. By day 13-15, AMS had completely reversed with 0% (0/26) of neurons being mechanically sensitive. The median conduction velocity of the neurons that developed AMS was 0.55 (IQR 0.26) m/s (n = 16), which was not significantly different from those that were not mechanically sensitive (combined median for 1-2, 4-5 and 8-9 days postoperative = 0.60 (0.26) m/s; n = 75; p = 0.34, Mann-Whitney test).

DISCUSSION

Our experiments show that inflammation of the axons of C/slow Aδ-fiber-neurons, which are likely to be nociceptors, causes transient ongoing activity that reaches a maximum on day 4-5 following induction and decreases to control levels after 2 weeks. The observation that vinblastine treatment does not evoke a statistically significant increase in ongoing activity at any postoperative point supports that inflammation is key to the development of axonal ongoing activity. Combined, these observations support that if undamaged peripheral nociceptors exhibit ongoing activity, there must be a persistent source of inflammation. The findings may be directly applicable to patients with persistent radiating pain, which may be due to focal inflammation anywhere along the clinically implicated peripheral nerve. The results also clearly demonstrate the vulnerability and adaptability of small diameter unmyelinated axons to subtle changes in their environment.

Since neuritis disrupts axonal transport, we have proposed that the cellular components necessary for the development of ongoing activity are transported by fast axonal transport and accumulate at the inflamed site. These cellular components might include immune receptors and/or ion channels, such as hyperpolarization activated channels, which have also been implicated in the mechanisms of ongoing activity (Emery et al. 2011; Richards and Dilley 2015; Weng et al. 2012). The lack of an increase in ongoing activity in A- or C-fiber neurons up to 15 days following vinblastine-induced axonal transport disruption is consistent with the necessity for inflammation to activate the altered axons; vinblastine is in fact anti-inflammatory by virtue of its anti-mitotic properties. Furthermore, the sensitivity of C-fiber axons following the direct application of noxious inflammatory chemicals to the vinblastine treatment site (Govea et al. 2017) is consistent with the immune-mediated activation of accumulated cellular components.

Data from this study add to the “peripheral generator” theory, which proposes that an ongoing or intermittent afferent barrage from nociceptors is required to maintain the cutaneous symptoms

320 associated with neuropathic pain (Campbell and Meyer 2006; Gracely et al. 1992; Woolf 2011; Xie et
321 al. 2005). The lack of increased ongoing activity from Aα/β- or C/slow Aδ-fiber neurons at any of the
322 examined time points following vinblastine treatment suggests that the previously reported tactile-
323 evoked cutaneous hypersensitivity in this model may be driven by AMS, since the time course of this
324 sensitivity is comparable to the hypersensitivity (Dilley et al. 2013).

325 The appearance and resolution of C-fiber AMS is consistent with the time course of slowed axonal
326 transport that we have shown in this model (Dilley et al. 2013). Axons that were mechanically
327 responsive were most likely nociceptors, since a high mechanical threshold was required to
328 stimulate the receptive fields. The time course of AMS contrasts from neuritis, where similar activity
329 persists beyond one month (Dilley and Bove 2008b). This difference most likely reflects the longer
330 duration of axonal transport disruption following neuritis (Dilley et al. 2013).

331 The transient development of neuritis-induced ongoing activity and AMS, and vinblastine-induced
332 AMS, contrasts from the reported chronicity in patients. In both models, altered nociceptor activity
333 occurs when there is an active peripheral stimulus. When the stimulus is absent, such as when
334 axonal transport has recovered and levels of specific inflammatory chemicals have resided (Pulman
335 et al. 2013), sensitivities resolve. These observations support that in patients, a peripheral stimulus,
336 such as inflammation, must be active to cause persistent and spontaneous pain, and movement-
337 evoked radiating pain. This hypothesis is consistent with MRI findings of possible nerve inflammation
338 in patients with chronic whiplash associated disorder (Greening et al. 2018), and also with the
339 persistent symptoms in a rat model of repetitive motion disorders, where neuritis is a prominent
340 feature (Barbe et al. 2013). Therefore, persistent nerve inflammation, due to injury to surrounding
341 soft tissues or direct irritation of the affected nerve, is a probable cause of prolonged focal axonal
342 transport disruption that may underlie altered nociceptor activity.

343 In summary, altered nociceptor activity may cause persistent and spontaneous pain (mainly through
344 the development of nociceptor ongoing activity) and radiating pain (through the development of

AMS). Many patients with these symptoms lack signs of nerve injury on routine clinical examination. In such patients, the underlying mechanisms may involve inflammation-induced axonal transport disruption. A detailed examination of ongoing activity following neuritis and vinblastine-induced axonal transport disruption has shown that neuritis causes the transient development of ongoing activity in C/slow Aδ-fiber neurons. The lack of ongoing activity in A- or C-fiber neurons at any of the examined time points following vinblastine treatment is consistent with the need for inflammation to drive ongoing activity. It also raises the question as to whether such activity is essential for the development of the associated cutaneous hypersensitivities. The present data also show that AMS develops rapidly following vinblastine treatment but is relatively short-lived. The present work adds to our understanding of the relative contributions of ectopic activity and reinforces the underestimated role of AMS in neuropathic pain mechanisms. It also supports that for pain to persist, an active stimulus that causes altered axonal transport, such as neuritis, must also persist. Concerning animal welfare, treating nerves with low doses of vinblastine provides a less severe model to examine the role of axonal transport disruption in neuropathic pain mechanisms. It avoids cutting nerves, which can lead to adverse effects, and allows axonal transport disruption along intact axons to be explored.

DECLARATION OF INTEREST

The authors declare there are no conflicts of interest regarding this work.

368 **ACKNOWLEDGMENTS**

369 This study was supported by the National Centre for the Replacement, Refinement and Reduction of
370 Animals in Research (NC/L00156X/1) and the Brighton and Sussex Medical School. Data created
371 during this research are openly available from the University of Sussex data archive at xxxxxxxxxx.

372

REFERENCES

Barbe MF, Gallagher S, Massicotte VS, Tytell M, Popoff SN, and Barr-Gillespie AE. The interaction of force and repetition on musculoskeletal and neural tissue responses and sensorimotor behavior in a rat model of work-related musculoskeletal disorders. *BMC Musculoskelet Disord* 14: 303, 2013.

Boucher TJ, Okuse K, Bennett DLH, Munson JB, Wood JN, and McMahon SB. Potent analgesic effects of GDNF in neuropathic pain states. *Science* 290: 124-127, 2000.

Bove GM, and Dilley A. The conundrum of sensitization when recording from nociceptors. *J Neurosci Methods* 188: 213-218, 2010.

Bove GM, Ransil BJ, Lin HC, and Leem JG. Inflammation induces ectopic mechanical sensitivity in axons of nociceptors innervating deep tissues. *J Neurophysiol* 90: 1949-1955, 2003.

Bove GM, Weissner W, and Barbe MF. Long lasting recruitment of immune cells and altered epi-perineurial thickness in focal nerve inflammation induced by complete Freund's adjuvant. *J Neuroimmunol* 2009.

Campbell JN, and Meyer RA. Mechanisms of neuropathic pain. *Neuron* 52: 77-92, 2006.

Chacur M, Milligan ED, Gazda LS, Armstrong C, Wang HC, Tracey KJ, Maier SF, and Watkins LR. A new model of sciatic inflammatory neuritis (SIN): induction of unilateral and bilateral mechanical allodynia following acute unilateral peri-sciatic immune activation in rats. *Pain* 94: 231-244, 2001.

Dilley A, and Bove GM. Disruption of axoplasmic transport induces mechanical sensitivity in intact rat C-fibre nociceptor axons. *J Physiol* 586: 593-604, 2008a.

Dilley A, and Bove GM. Resolution of inflammation-induced axonal mechanical sensitivity and conduction slowing in C-fiber nociceptors. *J Pain* 9: 185-192, 2008b.

Dilley A, and Greening J. Non-Specific Arm Pain. In: *Wall and Melzack's Textbook of Pain*, edited by McMahon S, and Koltzenburg MElsevier, 2012.

Dilley A, Greening J, Walker-Bone K, and Good C. Magnetic resonance imaging signal hyperintensity of neural tissues in diffuse chronic pain syndromes: a pilot study. *Muscle Nerve* 44: 981-984, 2011.

Dilley A, Lynn B, and Pang SJ. Pressure and stretch mechanosensitivity of peripheral nerve fibres following local inflammation of the nerve trunk. *Pain* 117: 462-472, 2005.

Dilley A, Richards N, Pulman KG, and Bove GM. Disruption of fast axonal transport in the rat induces behavioral changes consistent with neuropathic pain. *J Pain* 14: 1437-1449, 2013.

Dyck PJB, Engelstad J, Norell J, and Dyck PJ. Microvasculitis in non-diabetic lumbosacral radiculoplexus neuropathy (LSRPN): Similarity to the diabetic variety (DLSRPN). *J Neuropathol Exp Neurol* 59: 525-538, 2000.

Eliav E, Herzberg U, Ruda MA, and Bennett GJ. Neuropathic pain from an experimental neuritis of the rat sciatic nerve. *Pain* 83: 169-182, 1999.

Emery EC, Young GT, Berrocoso EM, Chen L, and McNaughton PA. HCN2 ion channels play a central role in inflammatory and neuropathic pain. *Science* 333: 1462-1466, 2011.

Fitzgerald M, Woolf CJ, Gibson SJ, and Mallaburn PS. Alterations in the structure, function, and chemistry of C fibers following local application of vinblastine to the sciatic nerve of the rat. *J Neurosci* 4: 430-441, 1984.

Govea RM, Barbe MF, and Bove GM. Group IV nociceptors develop axonal chemical sensitivity during neuritis and following treatment of the sciatic nerve with vinblastine. *J Neurophysiol* 118: 2103-2109, 2017.

Gracely RH, Lynch SA, and Bennett GJ. Painful neuropathy: altered central processing maintained dynamically by peripheral input. *Pain* 51: 175-194, 1992.

Greening J, Anantharaman K, Young R, and Dilley A. Evidence for increased MRI signal intensity and morphological changes in the brachial plexus and median nerves of patients with chronic arm and neck pain following whiplash injury. *J Orthop Sports Phys Ther* (In Press).

Janig W, and Baron R. Complex regional pain syndrome: mystery explained? *Lancet Neurol* 2: 687-697, 2003.

Kajander KC, Wakisaka S, and Bennett GJ. Spontaneous discharge originates in the dorsal root ganglion at the onset of a painful peripheral neuropathy in the rat. *Neurosci Lett* 138: 225-228, 1992.

Kashiba H, Senba E, Kawai Y, Ueda Y, and Tohyama M. Axonal blockade induces the expression of vasoactive intestinal polypeptide and galanin in rat dorsal root ganglion neurons. *Brain Res* 577: 19-28, 1992.

Katoh K, Tohyama M, Noguchi K, and Senba E. Axonal flow blockade induces alpha-CGRP mRNA expression in rat motoneurons. *Brain Res* 599: 153-157, 1992.

Loeser JD. Pain due to nerve injury. *Spine* 10: 232-235, 1985.

Pulman KG, Smith M, Mengozzi M, Ghezzi P, and Dilley A. The erythropoietin-derived peptide ARA290 reverses mechanical allodynia in the neuritis model. *Neuroscience* 233: 174-183, 2013.

Richards N, Batty T, and Dilley A. CCL2 has similar excitatory effects to TNF-alpha in a subgroup of inflamed C-fiber axons. *J Neurophysiol* 106: 2838-2848, 2011.

Richards N, and Dilley A. Contribution of hyperpolarization-activated channels to heat hypersensitivity and ongoing activity in the neuritis model. *Neuroscience* 284: 87-98, 2015.

Tal M, and Eliav E. Abnormal discharge originates at the site of nerve injury in experimental constriction neuropathy (CCI) in the rat. *Pain* 64: 511-518, 1996.

Waddell G. Clinical diagnosis of leg pain and nerve root involvement in low back disorders. *Acta Orthop Belgica* 53: 152-155, 1987.

Waddell PJ, Lawson SN, and McCarthy PW. Conduction velocity changes along the processes of rat primary sensory neurons. *Neuroscience* 30: 577-584, 1989.

Weng X, Smith T, Sathish J, and Djouhri L. Chronic inflammatory pain is associated with increased excitability and hyperpolarization-activated current (Ih) in C- but not Adelta-nociceptors. *Pain* 153: 900-914, 2012.

Woertgen C, Holzschuh M, Rothoerl RD, and Brawanski A. Clinical signs in patients with brachialgia and sciatica: a comparative study. *Surg Neurol* 49: 210-214, 1998.

Woolf CJ. Central sensitization: implications for the diagnosis and treatment of pain. *Pain* 152: S2-15, 2011.

Xie W, Strong JA, Meij JT, Zhang JM, and Yu L. Neuropathic pain: early spontaneous afferent activity is the trigger. *Pain* 116: 243-256, 2005.

Zager EL, Pfeifer SM, Brown MJ, Torosian MH, and Hackney DB. Catamenial mononeuropathy and radiculopathy: a treatable neuropathic disorder. *J Neurosurg* 88: 827-830, 1998.

Zhuo H, Lewin AC, Phillips ET, Sinclair CM, and Helke CJ. Inhibition of axoplasmic transport in the rat vagus nerve alters the numbers of neuropeptide and tyrosine hydroxylase messenger RNA-containing and immunoreactive visceral afferent neurons of the nodose ganglion. *Neuroscience* 66: 175-187, 1995.

FIGURE LEGENDS

Fig. 1. Conduction velocities of C- and A-fiber neurons. (A, B) Histogram of the conduction velocities of (A) C/slow Aδ- and (B) Aα/β-fiber neurons for each group. (C, D) Median conduction velocities of (C) C/slow Aδ- and (D) Aα/β -fiber neurons for each group at different postoperative time points. Saline-treated animals were only examined at 3-4 hours postoperative and on days 4-5. The number of C/slow Aδ- and Aα/β-fiber neurons in each group at each time point ranged from 72 to 147. C/slow Aδ-fiber neurons were characterized by electrical stimulation of the L5 dorsal root (see Fig. 2), whereas Aα/β-fiber neurons were characterized by electrical stimulation of the sciatic nerve (see Fig. 3). * $p < 0.05$, ** $p < 0.01$, *** $p < 0.001$, **** $p < 0.0001$ compared to untreated; ††† $p < 0.001$, †††† $p < 0.0001$ compared to saline treatment (Kruskal-Wallis test followed by Dunn's post hoc test). Error bars = IQR.

Fig. 2. Development of ongoing activity in C/slow Aδ- fiber neurons. (A) The percentage of ongoing activity is shown for the untreated, saline-treated, vinblastine-treated and neuritis groups at different postoperative time points. Numbers of neurons with ongoing activity are given. A schematic of the electrophysiology set-up is also shown. The recording (Rec) and stimulating (stim) sites at the L5 dorsal root are indicated. The treatment site is shown along the sciatic nerve in the mid-thigh (greyed area). *** $p < 0.001$ (Fisher's exact test). (B) Typical patterns of ongoing activity. Inserts: expanded waveforms.

Fig. 3. Development of ongoing activity in Aα/β-fiber neurons were characterized by electrical stimulation of the L5 dorsal root (see Fig. 2), whereas A-fiber neurons were characterized by electrical stimulation of the sciatic nerve (see Fig. 3).-fiber neurons. (A) The percentage of ongoing activity is shown for the untreated, saline-treated, vinblastine-treated and neuritis groups at different time points postoperative. Numbers of ongoing neurons are given. A schematic of the electrophysiology set-up is also shown. The recording site at the L5 dorsal root is indicated (Rec). The nerve was stimulated along the sciatic nerve in the mid-thigh (Stim), immediately distal to the treatment site (greyed area). (B) Typical patterns of ongoing activity. Ongoing spindles are also present in the untreated and neuritis traces (smaller units). Insert: expanded waveforms.

Fig. 4. Development of axonal mechanical sensitivity in C/slow Aδ- fiber neurons. (A) The percentage of AMS in deep and cutaneous (denoted by D and C respectively) innervating neurons is shown for the untreated group and the vinblastine-treated groups at different time points postoperative. Horizontal lines indicate the combined percentage of axons with mechanical sensitivity for deep and cutaneous innervating neurons. Numbers of neurons with AMS innervating deep and cutaneous structures are given. A schematic of the electrophysiology set-up is also shown. The recording (Rec) and stimulating (Stim) sites at the L5 dorsal root are indicated. The treatment site is shown along the sciatic nerve in the mid-thigh (greyed area). A notched platform was positioned under the treatment site to support the nerve during AMS testing. *$p<0.05$, ** $p<0.01$ compared to untreated, for percent of neurons innervating deep structures (Fisher's exact test). † $p<0.05$, †† $p<0.01$ compared to untreated, for all neurons (combined deep + cutaneous). (B) The response pattern of AMS is linked to the mechanical stimulus. Horizontal lines above trace represent the duration of the mechanical stimuli. Inserts: expanded waveforms.

506 **TABLES**

507 **Table 1. Rates (Hz) of ongoing activity in C/slow Aδ- and A- fiber neurons.**

		C/slow Aδ- fiber neurons		A-fiber neurons	
Treatment	**Time PO**	**Median**	**IQR**	**Median**	**IQR**
Untreated	0	0.60	1.03	0.02	0.00
Vinblastine	3-4hr	0.35	0.62	0.14	0.28
	1-2d	0.17	0.28	0.11	0
	4-5d	0.26	0.48	0.04	0.08
	12-15d	0.08	0.54	0.24	0.03
Neuritis	3-4hr	0.11	0.19	0.04	0.01
	1-2d	1.27*	1.31	0.09	0.17
	4-5d	0.55†#	1.53	0.11	0.09
	12-15d	0.10	0.13	0.02	0.00
Saline	3-4hr	0.14	0.10	0.03	0.15
	4-5d	0.47	0.56	0.21	0.20

508 * $p < 0.05$ compared to 3-4 hours and 12-15 days postoperative ; † $p < 0.05$ compared to 3-4 hours
509 postoperative (Kruskal-Wallis test followed by Dunn's post hoc tests). # Based on 20 neurons (Rate
510 could not accurately be determined for one neuron). PO postoperative, hr = hour, d = day.

511

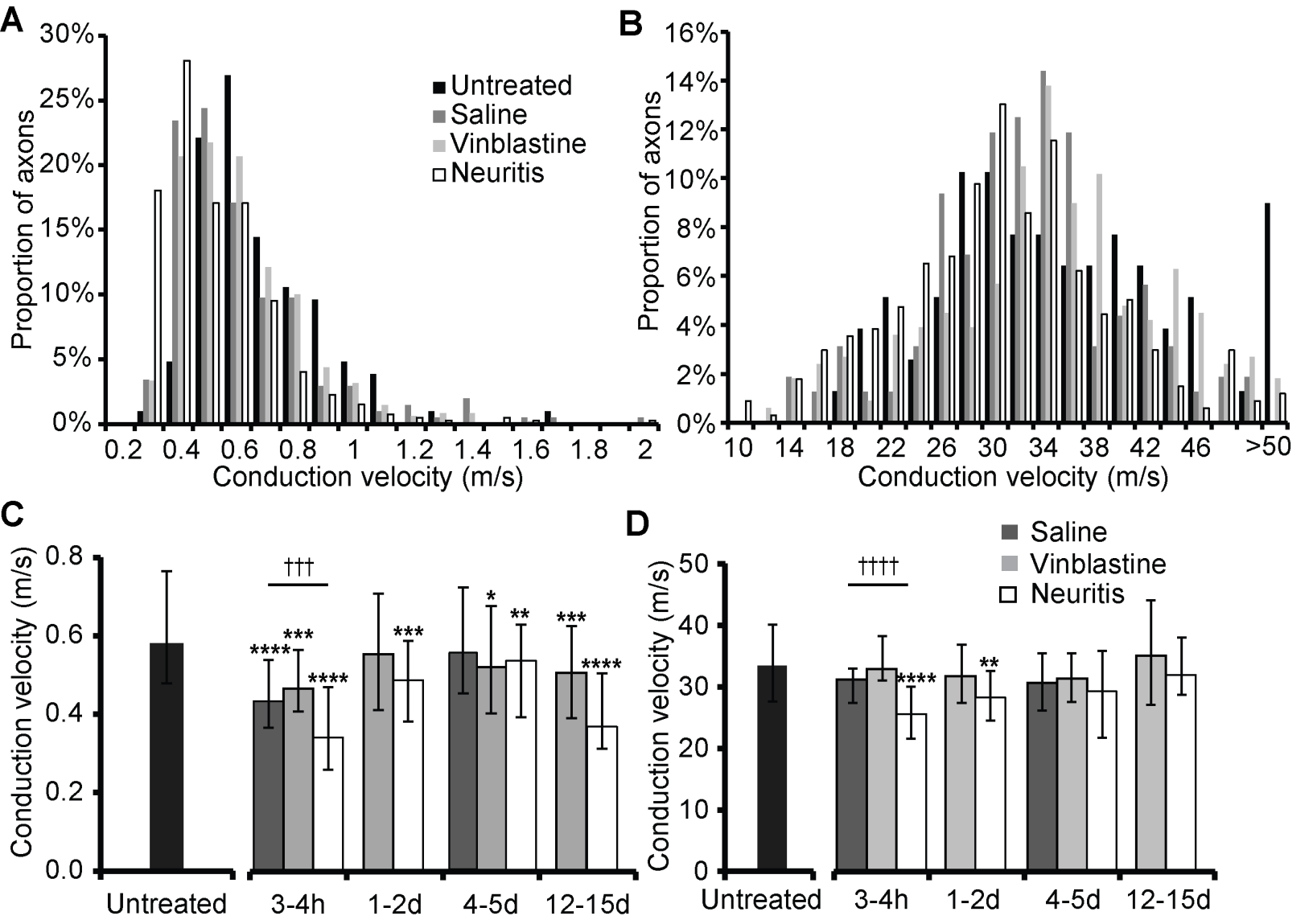
A
30%
25%
20%
15%
10%
5%
0%
Proportion of axons
Untreated
Saline
Vinblastine
Neuritis
0.2
0.4
0.6
0.8
1
1.2
1.4
1.6
1.8
2
Conduction velocity (m/s)
B
16%
14%
12%
10%
8%
6%
4%
2%
0%
Proportion of axons
10
14
18
22
26
30
34
38
42
46
>50
Conduction velocity (m/s)
C
Conduction velocity (m/s)
0.8
0.6
0.4
0.2
0.0
†††
****
***
****
***
*
**
***
****
Untreated
3-4h
1-2d
4-5d
12-15d
D
Saline
Vinblastine
Neuritis
Conduction velocity (m/s)
50
40
30
20
10
0
††††
****
**
Untreated
3-4h
1-2d
4-5d
12-15d

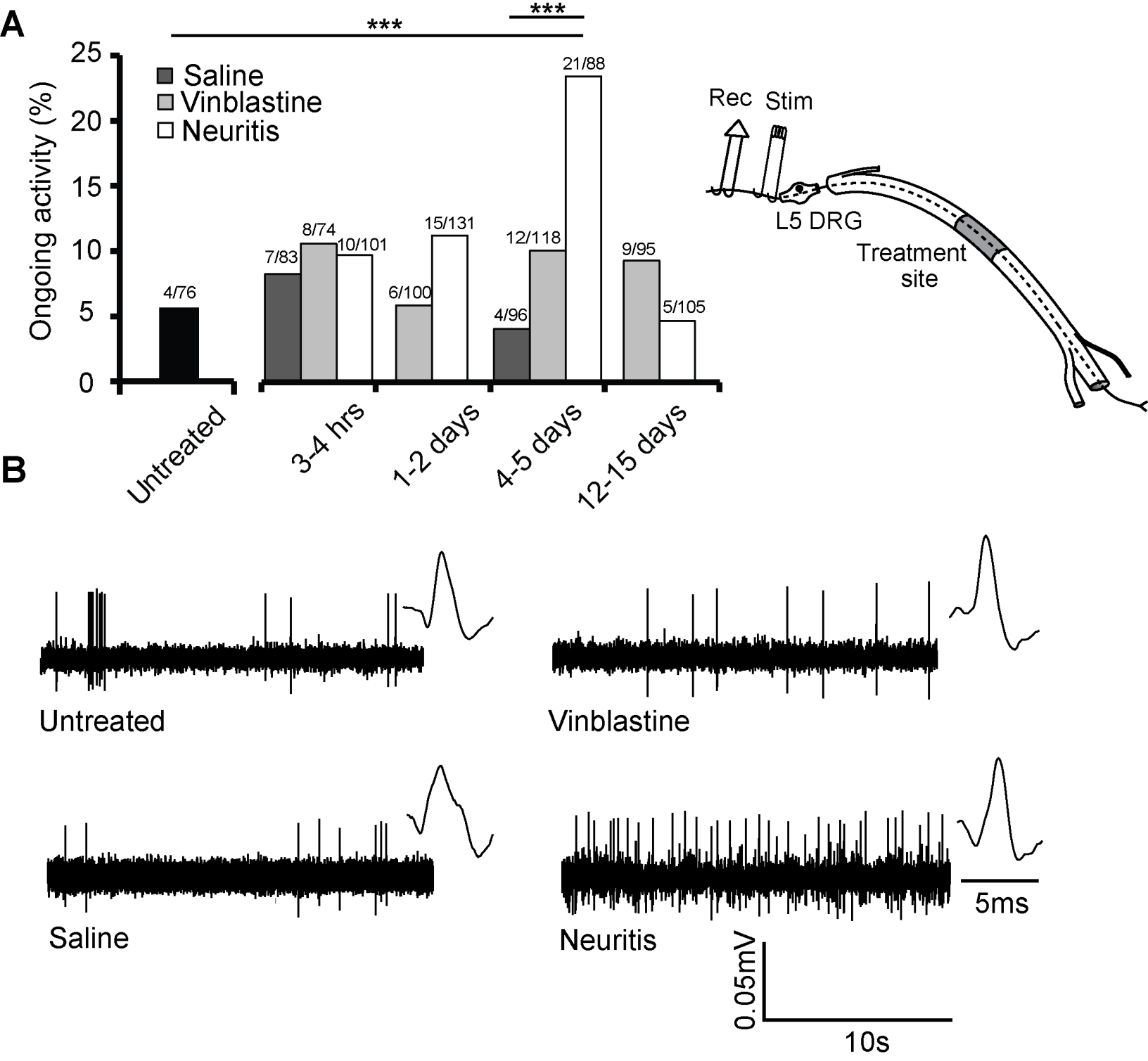
A
***
***
Saline
Vinblastine
Neuritis
Ongoing activity (%)
25
20
15
10
5
0
4/76
7/83
8/74
10/101
6/100
15/131
4/96
12/118
21/88
9/95
5/105
Untreated
3-4 hrs
1-2 days
4-5 days
12-15 days
Rec
Stim
L5 DRG
Treatment site
B
Untreated
Vinblastine
Saline
Neuritis
5ms
0.05mV
10s

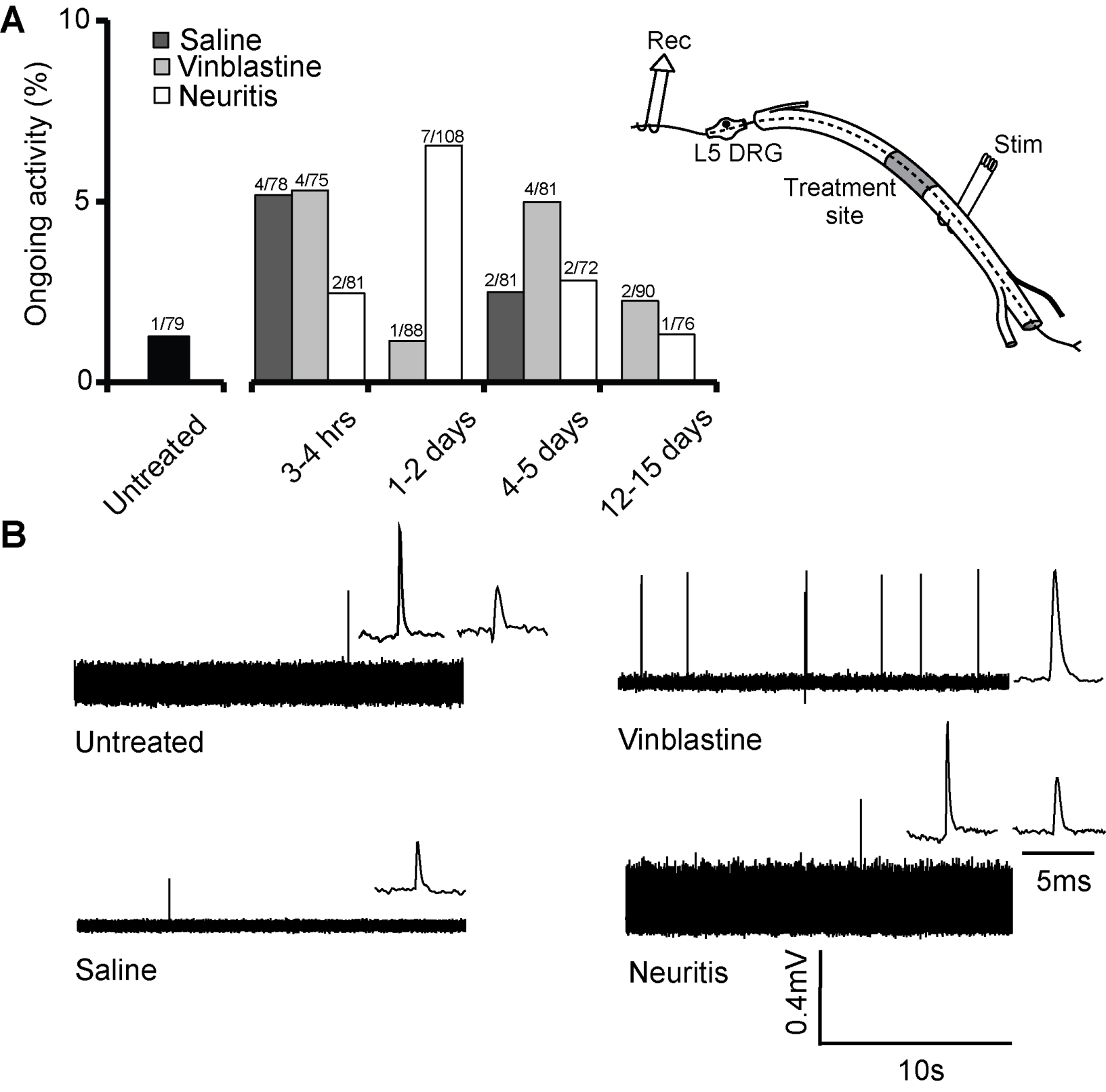
A
10
5
0
Ongoing activity (%)
Saline
Vinblastine
Neuritis
1/79
4/78
4/75
2/81
1/88
7/108
2/81
4/81
2/72
2/90
1/76
Untreated
3-4 hrs
1-2 days
4-5 days
12-15 days
Rec
L5 DRG
Treatment site
Stim
B
Untreated
Saline
Vinblastine
Neuritis
5ms
0.4mV
10s

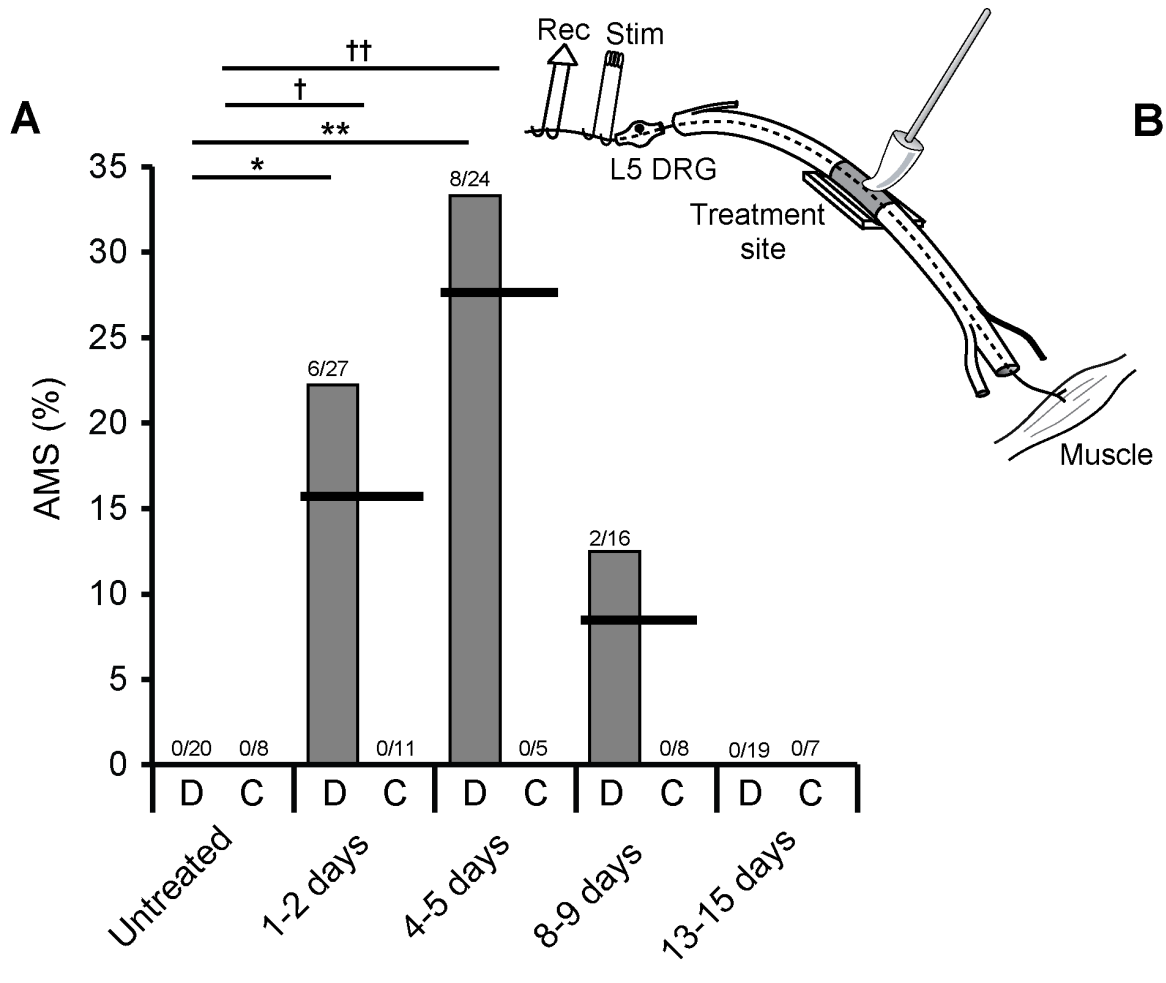
A
††
†
**
*
Rec
Stim
L5 DRG
Treatment site
Muscle
AMS (%)
35
30
25
20
15
10
5
0
8/24
6/27
2/16
0/20
0/8
0/11
0/5
0/8
0/19
0/7
D
C
Untreated
1-2 days
4-5 days
8-9 days
13-15 days

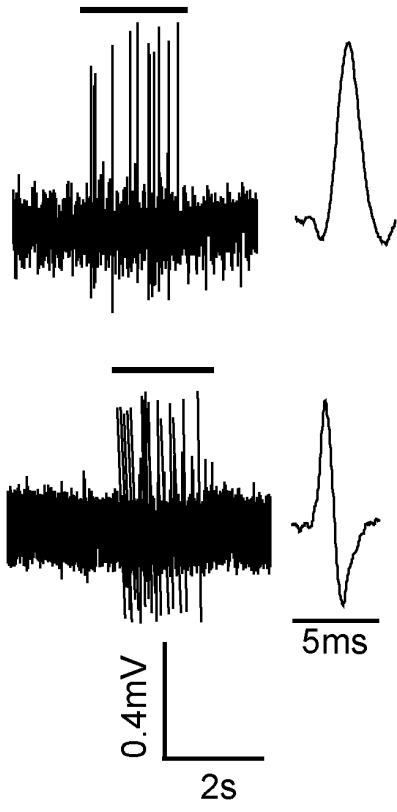
B
5ms
0.4mV
2s